Signal Analysis by Generalized Hilbert Transforms on the Unit Sphere

Lennart Wietzke, Oliver Fleischmann and Gerald Sommer

Institute of Computer Science, Chair of Cognitive Systems, Christian-Albrechts-University of Kiel, Germany

Abstract. In 1D signal processing *local energy* and *phase* can be determined by the *analytic signal*. *Local energy*, *phase* and *orientation* of 2D signals can be analyzed by the *monogenic signal* for all *i(ntrinsic)1D* signals in an *rotational invariant* way by the *generalized Hilbert transform*. In order to analyze both i1D and i2D signals in one framework the main idea of this contribution is to lift up 2D signals to the higher dimensional *conformal space* in which the original signal can be analyzed with more degrees of freedom by the *generalized Hilbert transform* on the unit sphere. An appropriate embedding of 2D signals on the unit sphere results in an extended feature space spanned by local *energy*, *phase*, *orientation/direction* and *curvature*. In contrast to classical differential geometry, local curvature can now be determined by the generalized Hilbert transform in *monogenic scale space* without any derivatives.

INTRODUCTION

In 1D signal processing the *local energy* and *phase* can be determined by the *analytic signal* [1] and the Hilbert transform [2]. The *local energy*, *1D phase* and *orientation* of 2D signals $f \in L_2(\mathbb{R}^2; \mathbb{R})$ can be analyzed by the *monogenic signal* [3] for all *i(ntrinsic)1D* signals in an *rotational invariant* way by the *generalized Hilbert transform* (first order 2D Riesz transform in Euclidean space) known from Clifford analysis [4].

In order to analyze both i1D and i2D signals in one framework the main idea of this paper is to lift up 2D signals to higher dimensional *conformal spaces* (see [5] and [6]) in which the original signal can be analyzed with more degrees of freedom by the *generalized Hilbert transform* on the unit sphere [7]. An appropriate embedding of 2D signals on the unit sphere results in an extended feature space spanned by local energy, phase, orientation/direction and *curvature*. In contrast to classical differential geometry, local curvature can now be determined by the generalized Hilbert transform in *monogenic scale space* [8] without any derivatives. This novel approach contains the monogenic signal as a special case for i1D signals with zero curvature. Further advantages are the low computational time complexity of a 2D convolution, the easy implementation without Fourier transformation in spatial domain and the advantages of phase based signal processing now with respect to curvature, i.e. the local curvature is independent of the local energy which is very important for local signal analysis.

GENERALIZED HILBERT TRANSFORMS ON $\mathbb{S}^n$

The generalized Hilbert transform on the unit sphere $\mathbb{S}^n := \left\{ v \in \mathbb{R}^{n+1} : \|v\| = 1 \right\}$ can be defined according to [4] by

$$H\{c\}(\xi) = \frac{2}{A_{n+1}} \text{P.V.} \int_{\omega \in \mathbb{S}^n} \frac{(\xi - \omega) \circ \omega}{\|\xi - \omega\|^{n+1}} c(\omega) \, dS(\omega) \tag{1}$$

with $\circ$ as the geometric product and $\xi \in \mathbb{S}^n$, A_{n+1} as the surface area and dS as the surface element of the unit sphere $\mathbb{S}^n$. In order to evaluate the Hilbert transform of the original signal f on $\mathbb{S}^2$ the original signal f will be embedded on $\mathbb{S}^2$ by projecting $\mathbb{R}^2$ to $\mathbb{S}^2$. The conformal mapping is given by

$$\mathscr{C}(x, y) := \frac{1}{x^2 + y^2 + 1} \begin{bmatrix} 2x \\ 2y \\ x^2 + y^2 - 1 \end{bmatrix} \tag{2}$$

and its inversion [9] is given by

$$\mathscr{C}^{-1}(\omega) := \frac{1}{1-\omega_3} \begin{bmatrix} \omega_1 \\ \omega_2 \end{bmatrix} \tag{3}$$

with $\omega := (\omega_1, \omega_2, \omega_3)$. This results in the conformal embedding of the original 2D planar signal

$$c(\omega) := \begin{cases} f(\mathscr{C}^{-1}(\omega)^T) & , \omega \in \mathbb{S}^2 - \{(0,0,1)\} \\ 0 & , \text{else} \end{cases} . \tag{4}$$

With $\xi \in \mathbb{S}^2$ and $\xi := (0,0,-1)$ (south pole of the sphere) as the origin of the local coordinate system relatively to the test point of local interest, the components of the singular integral (1) can be analyzed by the evaluation of the geometric product of the two vectors $\omega = \omega_1 \mathbf{e}_1 + \omega_2 \mathbf{e}_2 + \omega_3 \mathbf{e}_3$ and $\xi = \xi_1 \mathbf{e}_1 + \xi_2 \mathbf{e}_2 + \xi_3 \mathbf{e}_3 = -\mathbf{e}_3$

$$(\xi - \omega) \circ \omega = 1 + \omega_1 \mathbf{e}_{13} + \omega_2 \mathbf{e}_{23} + \omega_3 \tag{5}$$

and evaluating

$$\|\xi - \omega\|^3 = \sqrt{2+2\omega_3}^3 \tag{6}$$

with the norm of a vector $\|x\| := \sqrt{\sum_{i=1}^{n} x_i^2}$ and $\omega = \sum_{i=1}^{3} \omega_i \mathbf{e}_i$ in vector notation of the Clifford algebra. Plugging these results into equation (1) and evaluating it at the origin $\xi = (0,0,-1)$ results in

$$H\{c\}(\xi) = \underbrace{\frac{2}{A_3} \text{P.V.} \int_{\omega \in \mathbb{S}^2} \frac{1}{\sqrt{2+2\omega_3}^3} c(\omega)\, dS(\omega)}_{=:H_0\{c\}(\xi)} + \underbrace{\frac{2}{A_3} \text{P.V.} \int_{\omega \in \mathbb{S}^2} \frac{\omega_1}{\sqrt{2+2\omega_3}^3} c(\omega)\, dS(\omega) \mathbf{e}_{13}}_{=:H_1\{c\}(\xi)\mathbf{e}_{13}} \tag{7}$$

$$+ \underbrace{\frac{2}{A_3} \text{P.V.} \int_{\omega \in \mathbb{S}^2} \frac{\omega_2}{\sqrt{2+2\omega_3}^3} c(\omega)\, dS(\omega) \mathbf{e}_{23}}_{=:H_2\{c\}(\xi)\mathbf{e}_{23}} + \underbrace{\frac{2}{A_3} \text{P.V.} \int_{\omega \in \mathbb{S}^2} \frac{\omega_3}{\sqrt{2+2\omega_3}^3} c(\omega)\, dS(\omega)}_{=:H_3\{c\}(\xi)} . \tag{8}$$

The signal model in conformal space will be a great circle with azimuthal orientation angle θ. The Hilbert transform on $\mathbb{S}^2$ can be used to determine all features that can be determined by the Riesz transform in real analysis. But the Hilbert transform on $\mathbb{S}^2$ provides a new way of interpretation in contrast to the real Radon domain [10]. This will be shown by comparison of the Riesz transform $R_j\{\cdot\}$ and the Hilbert transform $H_j\{\cdot\}$ on the sphere. Recalling that the transforms evaluated at $\xi = (0,0,-1)$ with $x = (x_1, x_2, x_3) := r\omega \in \mathbb{R}^3$ and $r \in \mathbb{R}$ read

$$R_j\{c\}(\xi) = \frac{2}{A_4} \text{P.V.} \int_{x \in \mathbb{R}^3} \frac{x_j}{\|x - \xi\|^4} c(x)\, dx = \frac{2}{A_4} \text{P.V.} \int_{\omega \in \mathbb{S}^2} \frac{\omega_j}{\sqrt{2+2\omega_3}^4} c(\omega)\, dS(\omega) \tag{9}$$

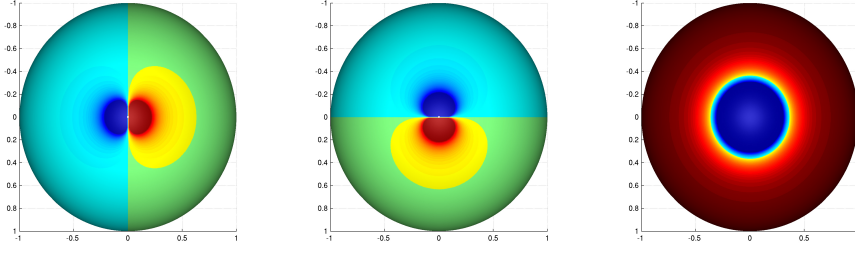$$H_j\{c\}(\xi) = \frac{2}{A_3} \text{P.V.} \int_{\omega \in \mathbb{S}^2} \frac{\omega_j}{\sqrt{2+2\omega_3}^3} c(\omega)\, dS(\omega) . \tag{10}$$

Using the fact that $c(x)$ has only non-zero values for $x \in \mathbb{S}^2$ it is possible to restrict $c(x)$ to the set $\{x : 0 \leqslant \|x\| \leqslant 1\}$ and rewrite the integral of the Riesz transform as (see [11])

$$R_j\{c\}(\xi) = \frac{2}{A_4} \text{P.V.} \int_{0 \leqslant \|x\| \leqslant 1} \frac{x_j}{\|x - \xi\|^4} c(x)\, dx \tag{11}$$

$$= \frac{2}{A_4} \text{P.V.} \int_{r \in [0,1]} r^2 \left[\int_{\omega \in \mathbb{S}^2} \frac{\omega_j}{\sqrt{2+2\omega_3}^4} c(r\omega)\, dS(\omega) \right] dr \tag{12}$$

$$= \frac{2}{A_4} \text{P.V.} \int_{\omega \in \mathbb{S}^2} \frac{\omega_j}{(2+2\omega_3)^2} c(\omega)\, dS(\omega) . \tag{13}$$

FIGURE 1. From left to right: Visualization of the convolution kernels in x_1, x_2 and x_3 direction in spatial domain.

Since both transforms are equal up to the factor $\sqrt{2+2\omega_3}^{-1}$, the R_j kernels are characterized by a *faster decay* and rise towards the south pole. In order to obtain the same results as the 3D Riesz transform restricted to $\mathbb{S}^2$, the Hilbert transform on $\mathbb{S}^3$ will be considered now. Since $\mathbb{S}^2 \subset \mathbb{S}^3$ the embedding $\tilde{\omega} := (\tilde{\omega}_1, \tilde{\omega}_2, \tilde{\omega}_3, \tilde{\omega}_4) := (\omega_1, \omega_2, \omega_3, 0) \in \mathbb{S}^3$ with $\omega \in \mathbb{S}^2$ will be used. The signal c is now embedded as

$$\tilde{c}(\tilde{\omega}) := \begin{cases} c(\tilde{\omega}_1, \tilde{\omega}_2, \tilde{\omega}_3) & , \tilde{\omega}_4 = 0 \\ 0 & , \text{else} \end{cases}. \tag{14}$$

Using definition (1) with $n = 3$ and equations (5) and (6) extended to $n = 3$ yields the Hilbert transform on $\mathbb{S}^3$ evaluated at the origin $\tilde{\xi} := (0, 0, -1, 0)$ as

$$H\{\tilde{c}\}(\tilde{\xi}) = \underbrace{\frac{2}{A_4}\text{P.V.} \int\limits_{\omega \in \mathbb{S}^3} \frac{1}{(2+2\omega_3)^2} \tilde{c}(\omega)\, dS(\omega)}_{H_0\{\tilde{c}\}(\tilde{\xi})} + \underbrace{\frac{2}{A_4}\text{P.V.} \int\limits_{\omega \in \mathbb{S}^3} \frac{\omega_1}{(2+2\omega_3)^2} \tilde{c}(\omega)\, dS(\omega)\, \mathbf{e}_{14}}_{H_1\{\tilde{c}\}(\tilde{\xi})} \tag{15}$$

$$+ \underbrace{\frac{2}{A_4}\text{P.V.} \int\limits_{\omega \in \mathbb{S}^3} \frac{\omega_2}{(2+2\omega_3)^2} \tilde{c}(\omega)\, dS(\omega)\, \mathbf{e}_{24}}_{H_2\{\tilde{c}\}(\tilde{\xi})} + \underbrace{\frac{2}{A_4}\text{P.V.} \int\limits_{\omega \in \mathbb{S}^3} \frac{\omega_3}{(2+2\omega_3)^2} \tilde{c}(\omega)\, dS(\omega)}_{H_3\{\tilde{c}\}(\tilde{\xi})} \tag{16}$$

$$+ \underbrace{\frac{2}{A_4}\text{P.V.} \int\limits_{\omega \in \mathbb{S}^3} \frac{\omega_4}{(2+2\omega_3)^2} \tilde{c}(\omega)\, dS(\omega)\, \mathbf{e}_{34}}_{H_4\{\tilde{c}\}(\tilde{\xi})}. \tag{17}$$

Since $\omega_4 = 0 \ \forall \omega \in \mathbb{S}^3$ with $\tilde{c}(\omega) \neq 0$ due to the nature of the embedding it follows that $H_4\{\tilde{c}\}(\tilde{\xi}) = 0$. Furthermore, considering spherical coordinates

$$\omega = \sin\varphi \cos\theta \mathbf{e}_1 + \sin\varphi \sin\theta \cos\gamma \mathbf{e}_2 + \cos\theta \mathbf{e}_3 + \sin\varphi \sin\theta \sin\gamma \mathbf{e}_4 \tag{18}$$

in $\mathbb{S}^3$ and using the fact that $\omega_4 = 0$ where $\tilde{c}(\omega) \neq 0$, it follows that $\gamma = 0$. Therefore, the result is the following equivalence of the generalized Hilbert transform on the unit sphere and the Riesz transform in conformal space

$$H_j\{\tilde{c}\}(\tilde{\xi}) = R_j\{c\}(\xi), \quad j \in \{1, 2, 3\} \tag{19}$$

at the origin $\xi = (0, 0, -1)$ and $\tilde{\xi} = (0, 0, -1, 0)$ (south pole of the sphere) of the local coordinate system for each test point.

CONCLUSION

It has been shown that the Riesz transform in $\mathbb{R}^3$ for the restriction to the sphere $\mathbb{S}^2$ and the Hilbert transform on $\mathbb{S}^3$ are equivalent. This results in a generalized isotropic *analytic signal* for 2D signals called the *conformal monogenic*

signal

$$f_{\text{CMS}}(\tilde{\xi}) = \begin{bmatrix} \tilde{c}(\tilde{\xi}) \\ H_1\{\tilde{c}\}(\tilde{\xi}) \\ H_2\{\tilde{c}\}(\tilde{\xi}) \\ H_3\{\tilde{c}\}(\tilde{\xi}) \end{bmatrix} \tag{20}$$

which can be evaluated at the south pole $\tilde{\xi} = (0,0,-1,0)$ relatively to each local test point. In [6] and [5] it is shown how to extract features such as phase, orientation, energy and curvature from the *conformal monogenic signal*. This approach can be extended to any dimension. Analysis of data defined on the unit sphere $\mathbb{S}^n$ is important in various signal processing fields like geoscience and processing of images captured by catadioptric cameras. Therefore, it is worth investigating the Hilbert transform on $\mathbb{S}^n$ in order to obtain features which are naturally arising on the sphere.

ACKNOWLEDGMENTS

REFERENCES

1. D. Gabor, *Journal IEE* **93**, 429–457 (1946).
2. S. L. Hahn, *Hilbert Transforms in Signal Processing*, Artech House Inc, Boston, London, 1996.
3. M. Felsberg, and G. Sommer, *IEEE Transactions on Signal Processing* **49**, 3136–3144 (2001).
4. R. Delanghe, *Bull. Belg. Math. Soc. Simon Stevin* **11**, 163–180 (2004).
5. L. Wietzke, O. Fleischmann, and G. Sommer, "2D Image Analysis by Generalized Hilbert Transforms in Conformal Space," in *ECCV*, LNCS, Springer-Verlag, Berlin, Heidelberg, New York, 2008.
6. L. Wietzke, and G. Sommer, "The Conformal Monogenic Signal," in *Pattern Recognition*, edited by G. Rigoll, Springer-Verlag, Berlin, Heidelberg, New York, 2008, vol. 5096 of *LNCS*, pp. 527–536.
7. F. Brackx, B. D. Knock, and H. D. Schepper, *International Journal of Mathematics and Mathematical Sciences* (2006).
8. M. Felsberg, and G. Sommer, *Journal of Mathematical Imaging and Vision* **21**, 5–26 (2004).
9. T. Needham, *Visual Complex Analysis*, Oxford University Press, Oxford, 1997.
10. L. Wietzke, G. Sommer, C. Schmaltz, and J. Weickert, "Differential Geometry of Monogenic Signal Representations," in *Robot Vision*, edited by G. Sommer, Springer-Verlag, Berlin, Heidelberg, New York, 2008, vol. 4931 of *LNCS*, pp. 454–465.
11. J. A. Baker, *The American Mathematical Monthly* **104**, 36–47 (1997).